C. R. Physique 15 (2014) 309–317

Contents lists available at ScienceDirect

Comptes Rendus Physique

www.sciencedirect.com

Ultra-high-energy cosmic rays / Rayons cosmiques d'ultra-haute énergie

Ultra-high-energy cosmic neutrinos: at 10^{15} eV energies and above

Neutrinos cosmiques d'ultra haute énergie : 10^{15} eV et au-delà

Shigeru Yoshida

Department of Physics, Graduate School of Science, Chiba University, Chiba 263-8522, Japan

ARTICLE INFO

Article history:
Available online 1 April 2014

Keywords:
Cosmic rays
Neutrino
Ultra high energy
Cosmic ray sources

Mots-clés :
Rayons cosmiques
Neutrino
Ultra-haute énergie
Sources des rayons cosmiques

ABSTRACT

The high-energy neutrino astronomy has finally bloomed. The discovery of the first 10^{15} eV (PeV or 10^6 GeV) neutrino events by the IceCube Collaboration followed by the dedicated search for 10^{12}–10^{15} eV events exhibited the evidence of an astrophysical neutrino flux. The estimated flux level is around $E^2\phi_{\nu_e+\nu_\mu+\nu_\tau} = 3\times10^{-8}$ GeV cm^{-2} s^{-1} sr^{-1}, consistent with the intensity expected from the energetics of extragalactic cosmic rays. The strong bound of neutrino flux in the 10^{18}-eV range, which amounts to $E^2\phi_{\nu_e+\nu_\mu+\nu_\tau} = 1.2\times10^{-7}$ GeV cm^{-2} s^{-1} sr^{-1} at 1×10^{19} eV provided by IceCube has reached the flux region predicted for some ultra-high-energy cosmic-ray source class candidates, leading to astrophysically meaningful constraints on the origin of cosmic rays. It disfavors strong cosmological evolution of the highest energy cosmic ray sources such as the Fanaroff–Riley type-II class of radio Galaxies. We live in an era when neutrinos provide clues to resolve long-standing mystery of ultra-high-energy cosmic rays.

RÉSUMÉ

L'astronomie neutrino est enfin ouverte. La découverte des premiers événements neutrino de 10^{15} eV (PeV ou 10^6 GeV) par la collaboration IceCube suivie d'une recherche fructueuse d'événements dans la gamme des 10^{12}–10^{15} eV a démontré l'existence d'un flux de neutrinos astrophysiques. Le flux est estimé à environ $E^2\phi_{\nu_e+\nu_\mu+\nu_\tau} = 3\times10^{-8}$ GeV cm^{-2} s^{-1} sr^{-1}, en accord avec l'intensité déduite du bilan énergétique des rayons cosmiques extragalactiques. Au-dessus de 10^{18} eV, la limite sévère obtenue par IceCube, $E^2\phi_{\nu_e+\nu_\mu+\nu_\tau} = 1.2\times10^{-7}$ GeV cm^{-2} s^{-1} sr^{-1} à 10^{19} eV, a atteint la région de flux prédite pour certaines classes de sources de rayons cosmiques d'ultra-haute énergie, fournissant ainsi des limites contraignantes du point de vue astrophysique sur l'origine des rayons cosmiques. Cette limite défavorise une forte évolution cosmologique de sources telles que celle des radio-galaxies Fanaroff–Riley de type II. Nous entrons dans l'ère où les neutrinos fournissent des indices pour résoudre le sempiternel mystère des rayons cosmiques.

E-mail address: syoshida@hepburn.s.chiba-u.ac.jp.

http://dx.doi.org/10.1016/j.crhy.2014.02.014

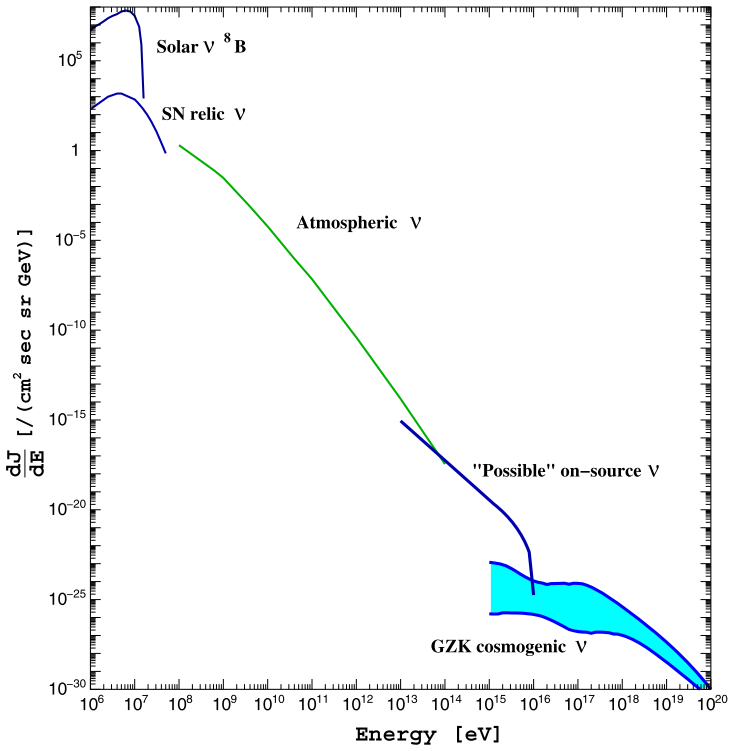

Fig. 1. (Color online.) Neutrino fluxes in the energy range above the MeV. Solar neutrinos from ^{8}B [1], supernova relic neutrino background [2], atmospheric neutrinos [3] are compiled, respectively. A possible on-source neutrino flux directly produced by cosmic-ray sources is drawn based on Ref. [4] with parameters consistent with the recent observations by IceCube. The ranges of GZK cosmogenic neutrino flux is displayed by a band sandwiched by the possibly minimal and maximal intensities based on Ref. [5] for illustrative purposes.

1. Introduction

Cosmic neutrinos are expected to be produced in the interactions of high-energy hadronic particles from cosmic accelerators with surrounding photons and matter. At PeV energies or greater (1 PeV $= 10^{15}$ eV), neutrinos are a unique tool for the direct survey of the ultra-high-energy universe, because at these energies photons are highly attenuated by the cosmic microwave background (CMB). In addition to neutrinos directly produced in cosmic-ray sources ("On-source" neutrinos), secondary neutrinos produced in the propagation of ultra-high-energy cosmic-rays (UHECRs) with energies reaching about 100 EeV (1 EeV $= 10^{3}$ PeV) are expected. These "cosmogenic" neutrinos are produced by the Greisen–Zatsepin–Kuzmin (GZK) mechanism via interactions of UHECRs with the CMB and extragalactic background light (infrared, optical, and ultraviolet) [6–8]. A measurement of cosmogenic (or GZK) neutrinos probes the origin of the UHECRs because the spectral shapes and flux levels are sensitive to the redshift dependence of UHECR source distributions and to the cosmic-ray primary compositions and injection spectrum [9,10]. Neutrinos are ideal particles to investigate the origin of UHECRs since neutrinos propagate to the Earth essentially without deflection and absorption. The main energy range of the cosmogenic neutrinos is predicted to be around 100 PeV–10 EeV [5,11]. In this extremely high-energy (EHE) region, cosmogenic production is considered the main source of cosmic neutrinos.

Fig. 1 shows a compilation of neutrino fluxes. The astrophysical neutrino flux is expected to be well above the atmospheric neutrino intensity in the PeV range. Yet its intensity is nearly 20 orders of magnitude lower than that of the atmospheric neutrinos measured by the standard underground neutrino detectors in the GeV range. The GZK cosmogenic neutrino flux, presumably dominant in the EeV energy range, is even lower. The ranges of predicted neutrino fluxes implies that the 4π solid angle averaged neutrino effective area (the total cross section of all targets in the detection volume) divided by energy A_ν/E must be larger than 10^{-5} m^2/GeV (e.g. $A_\nu \geqslant 10^{3}$ m^2 at 100 PeV and $A_\nu \geqslant 10^{4}$ m^2 at 1 EeV) to detect several ultra-high-energy (UHE) neutrinos every year.

Several techniques have been used to realize such huge detection volumes for these UHE neutrinos. Air-shower detectors search for neutrino-induced young inclined showers or Earth-skimming events initiated by tau neutrinos [12–14]. Radio Cherenkov neutrino detectors search for radio Askaryan pulses in a dielectric medium as the EHE neutrino signature [15–17]. Underground neutrino telescopes, such as the IceCube Neutrino Observatory [18], realized 1 km^3 or even larger detection volumes [19]. Together with its omni-directional neutrino detection capability, the IceCube is presently the most sensitive neutrino detector from the TeV to the EeV.

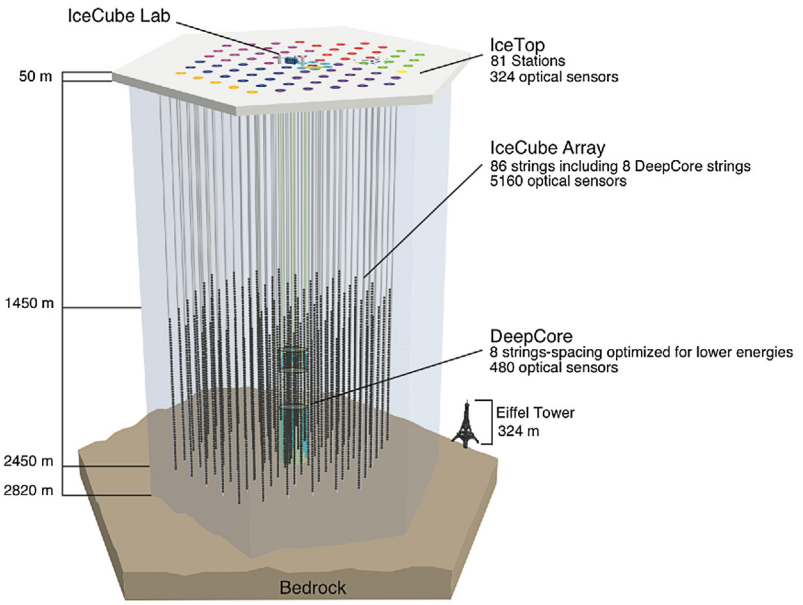

Fig. 2. (Color online.) A schematic view of the IceCube detector.

In this article, we review the present status of the UHE neutrino astronomy. The recent results from the IceCube experiments are highlighted. The results from the Auger experiment using the air-shower technique and the ANITA/RICE experiments implementing Radio Cherenkov detectors are followed to describe the various technique to cover the energy range above one EeV. The implications on the origin of UHECRs are finally discussed.

2. The results from the IceCube

2.1. The IceCube detector and the method to search for UHE neutrinos

The IceCube detector observes the Cherenkov light from the relativistic charged particles produced by high-energy neutrino interactions, using an array of Digital Optical Modules (DOMs). These DOMs are deployed along electrical cable bundles that carry power and information between the DOMs and the surface electronics. The cable assemblies, called strings, were lowered into holes drilled to a depth of 2450 m with a horizontal spacing of approximately 125 m (Fig. 2).

There are two classes of background events; atmospheric muon bundle events and events induced by atmospheric neutrinos. Muon bundles consist of a large number of high-energy muons produced by cosmic-ray interactions in the atmosphere. Regardless of their high muon multiplicities, they are observed as a single track since their lateral separations, of about 10 m, are shorter than the minimum DOM separation of 17 m. Both classes of background are simulated to estimate the total rate passing the final signal selection criteria. These background event simulations and their intensive comparisons with the real data ensure the reliability of the rare UHE neutrino-induced signal search.

The energy spectrum of atmospheric muons and neutrinos falls steeply with energy. The cosmogenic or astrophysical neutrino fluxes with their harder spectra are expected to dominate over this background at high energies, as illustrated in Fig. 1. Because the amount of deposited energy, i.e. the observable energy, is correlated with the energy of the incoming particles, the signal events stand out against the background events at high-energy. Therefore, the analysis is targeted towards the selection of these high energy events. The total number of photoelectrons (NPE) recorded in an event was used as the main distinctive feature to separate signal from background. The nearly proportional relation between the deposited energies inside the instrumentation volume and the amount of light from the Cherenkov radiation yields a clear correlation between NPE and the energy of the muons [19]. By selecting events with NPE above an appropriate threshold, low-energy events, dominated by atmospheric backgrounds, are filtered out.

The most recent results are based on two years of data taken from May 2010 to May 2012. The signal selection criteria were optimized based on simulations of background and signal, while the simulation was controlled using a test sample of the real data. The zenith-angle-dependent NPE threshold values were determined such that the model discovery potential [20,21] is maximized in each sample. For the 615.9 day life time, the expected numbers of background events from atmospheric muons and neutrinos from decays of pions and kaons in the final sample are $0.038 \pm 0.004(\text{stat})^{+0.021}_{-0.038}(\text{syst})$ and $0.021 \pm 0.001(\text{stat})^{+0:038}_{-0.007}(\text{syst})$, respectively. The major fraction of the systematic errors arises from the uncertainties on the flux and mass compositions of UHECRs and the optical properties of the glacier ice [19].

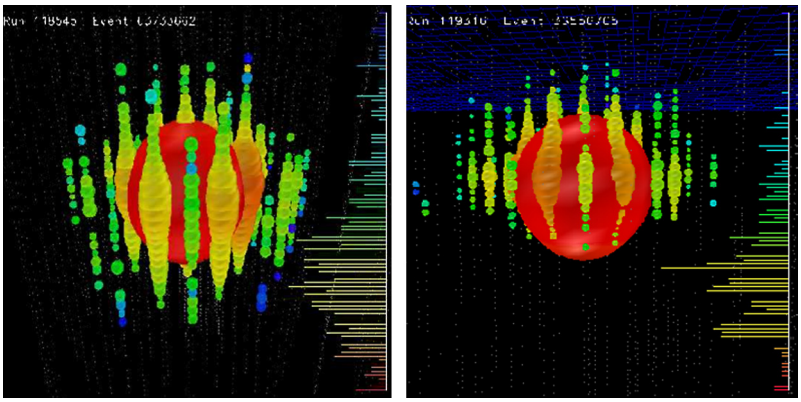

Fig. 3. The event displays of the two observed events from August 2011 (left panel) and January 2012 (right panel). Each sphere represents a DOM. Colors indicate the arrival timing of the photon (red = earliest, blue = latest). The sizes of the sphere indicates the measured amount of photons in each DOM. (For interpretation of the references to color in this figure legend, the reader is referred to the web version of this article.)

2.2. The detection of the PeV neutrinos

Two events passing the final selection criteria are observed [22]. The hypothesis that the two events are fully explained by atmospheric background including the baseline prompt atmospheric neutrino flux [23] has a p-value of 2.9×10^{-3} (2.8σ). The waveform profiles and the detector hit patterns of both events are consistent with that of Cherenkov photons from particle cascades induced by neutrinos well inside the IceCube instrumentation volume. There is no indication of outgoing/incoming muon or tau tracks. Event displays of the observed two events are shown in Fig. 3. This observation is the very first indication of the UHE astrophysical neutrinos.

The reconstructed *deposited* energies of the two observed cascades are 1.04 ± 0.16 PeV and 1.14 ± 0.17 PeV, respectively. The statistical energy resolutions for these events are obtained by simulating cascades with parameters close to the reconstructed energies and cascade vertices, and are found to be 3%. The total error on the energy is dominated by systematic uncertainties. These include the absolute detection efficiency of the DOM and the optical properties of the ice, both of which are major factors when relating the number of observed photons to the cascade energy. The sizes of the errors are estimated by reconstructing simulated events with various models of the ice properties.

The incoming neutrino energy corresponds exactly to the deposited cascade energy if a charged-current interaction of an electron neutrino induces a cascade. For neutral current reactions of neutrinos of any flavor, only a fraction of the neutrino energy is transferred to a cascade depending on the inelasticity of the collision. Including the hypothesis of neutral-current interaction of three flavors of neutrinos, the statistical error, and the systematic error, the 90% most probable neutrino energies of the two events at the earth surface are 810 TeV–7.6 PeV and 930 TeV–8.9 PeV, respectively, assuming that the surface neutrino spectrum follows an E^{-2} power law. Since the neutrino–nucleon interaction cross-section increases with neutrino energy, the possibility that the energy of the primary neutrino is much higher than the observed cascade energy is not entirely negligible, depending on the neutrino spectrum. For example, the 90% C.L. energy range for a cosmogenic neutrino model [24] extends to about 500 PeV, which shows that the reconstructed energy range heavily depends on the shape of the neutrino energy spectrum.

The IceCube results in the UHE range are characterized by two observational facts: the detection of two neutrinos with deposited energies of about one PeV and the non-detection of neutrinos with higher deposited energies. The detail tests have been conducted to conclude that none of the proposed cosmogenic neutrino models explains these two results. This rejection includes the cosmogenic model exhibiting an increased flux of neutrinos at PeV energies [25], due to assuming the "dip" transition model [26] of UHECRs and the stronger IR/UV background light.

The non-detection of neutrinos with deposited energies greater than a PeV yields the strong upper limit on the neutrino flux in the EeV range [19]. We discuss its implications on the UHECR origin in Section 6.

2.3. A follow-up search: evidence of extraterrestrial neutrinos

Although the UHE analysis had some sensitivity to neutrino events of all flavors above 1 PeV, it was mostly sensitive to ν_μ events above 10 PeV. A follow-up analysis designed to characterize the flux responsible for these events was performed by conducting an exploratory search for neutrinos at lower energies with interaction vertices well contained within the detector volume. Neutrino candidates were selected by finding events that originated within the detector interior. This selection does not rely on the topology of events, so that it is sensitive to all three flavors of neutrinos nearly equally. The outer detector array plays as a veto detector. The veto technique rejects 99.999% of the muon background at energies above a few hundred TeV. This rejection power was estimated by the tagged data sample without using the background-event simulation.

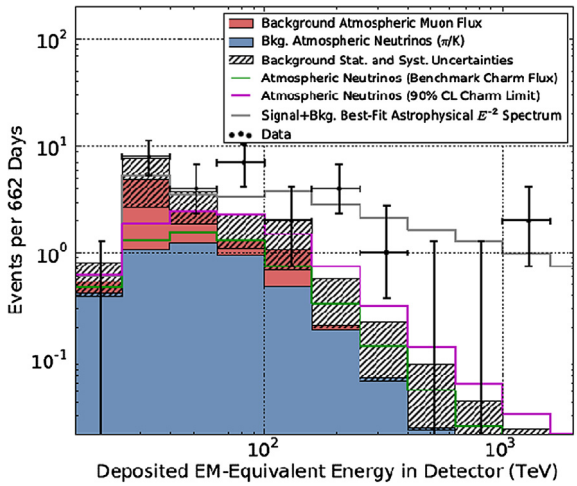

Fig. 4. Distribution of the deposited energies of the observed events compared to model predictions [27]. Energies plotted are reconstructed in-detector visible energies, which are lower limits on the neutrino energy. Note that deposited energy spectra are always harder than the spectrum of the neutrinos that produced them, due to the fact that the neutrino cross-section increases with energy. The expected rate of atmospheric neutrinos is shown in blue, with atmospheric muons in red. The green line shows our benchmark atmospheric neutrino flux, the magenta line the experimental 90% bound. The gray line shows the best-fit E^{-2} astrophysical spectrum with an all-flavor normalization of $E^2\phi_{\nu_e+\nu_\mu+\nu_\tau} = 3.6 \times 10^{-8}$ GeV cm^{-2} s^{-1} sr^{-1}. (For interpretation of the references to color in this figure legend, the reader is referred to the web version of this article.)

In the two-year dataset, 28 events with in-detector deposited energies between 30 and 1200 TeV were observed for an expected background of $10.6^{+5.0}_{-3.6}$ events from atmospheric muons and neutrinos [27]. The two most energetic of these are the previously detected PeV events in the UHE analysis. Seven events contained clearly identifiable muon tracks, while the remaining twenty-one were shower-like. Four of the low energy track-like events start near the detector boundary and are downgoing, which is consistent with the properties of the expected 6.0 ± 3.4 background atmospheric muons. The significance of the excess over atmospheric backgrounds was evaluated based on both the total rate and properties of the observed events. From each event, the total deposited PMT charge, reconstructed energy, and direction were used to compute tail probabilities relative to the atmospheric muon and neutrino backgrounds. The overall significance was computed using the product of the per-event probabilities as a test statistic. For the 26 events excluding the previously detected two PeV events, a background origin is rejected with a significance of 3.3σ. Combined by Fisher's method with the 2.8σ observation of the UHE analysis where the two highest-energy events were first reported, a final significance of 4.1σ is obtained for the entire data set of 28 events.

The observed events are much higher in energy, with a harder spectrum (Fig. 4) than expected from an extrapolation of the well-measured π/K atmospheric background at lower energies. The data are well described in the range 60 TeV $\leqslant E_{\rm dep} \leqslant$ 2 PeV by an E^{-2} neutrino spectrum with a three-flavor normalization of $E^2\phi_{\nu_e+\nu_\mu+\nu_\tau} = (3.6 \pm 1.2) \times 10^{-8}$ GeV cm^{-2} s^{-1} sr^{-1}. No statistically significant anisotropy was found, although the angular resolution of the shower event samples, dominating the population of the observed 28 events, is rather poor (10–20°).

A few remarks on these findings should be made. The estimated intensity of the high-energy neutrino streams is compatible with the Waxman–Bahcall bound [4]. This bound was obtained by assuming that sources of the highest-energy cosmic ray protons are also efficient neutrino emitters, with an optical depth of ~ 1. This fact would yield a great deal of clues on the properties of UHECR sources, if these neutrinos came from the extragalactic space. Many discussions along this line has already appeared in the literature. Second, concerning the present statistics, it is not certain yet whether the two PeV events belong to a subclass of the other sub-PeV events. They may have their own origin. Even if this is the case, the PeV flux should not extend well above the EeV range. The IceCube would have already seen an event(s) at energies of the order of the EeV if the intensity is O(10^{-8}) GeV cm^{-2} s^{-1} sr^{-1}.

3. The results from the Pierre Auger experiment

When a UHE neutrino enters the atmosphere and interacts with a nucleus, it produces an extensive air shower. A deep neutrino interaction in the air induces a deeply penetrating shower. It can be initiated at a depth of ~ 2000 g cm^{-2} or greater, while a regular UHECR interacting in the atmosphere gives rise to a shower with an electromagnetic component reaching its maximal development after a depth of the order of 800 g cm^{-2} and extinguishing gradually within the next 1000 g cm^{-2}. A UHE ν_τ that enters the Earth just below the horizon would yield other distinguishable signatures. These Earth-skimming neutrinos undergo charged-current interactions to produce a very penetrating τ lepton. When the interaction occurs sufficiently close to the Earth's surface, the τ lepton can escape to the atmosphere and decay in flight. This would in most cases give rise to an extensive air shower traveling nearly horizontal and in the upward direction for an ideal spherical Earth surface. The Pierre Auger Observatory, designed to detect extensive air showers induced by UHECRs,

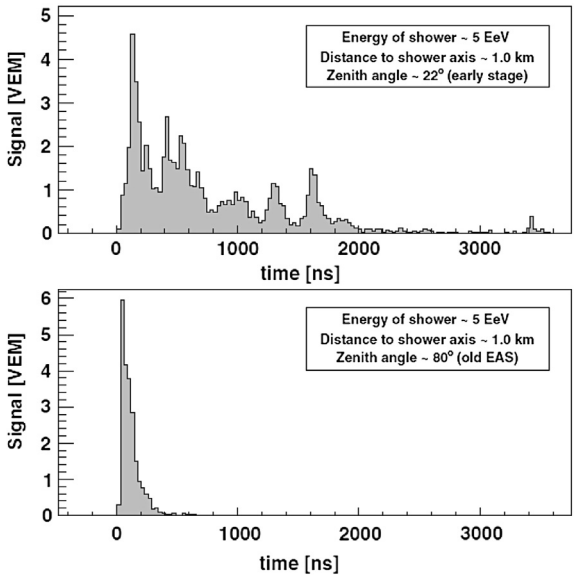

Fig. 5. FADC traces of stations at 1 km from the shower's core for two real shower events detected by the Auger surface detector array. Top panel: an example of signal profiles from early stages of shower development (zenith 22°); bottom: old extensive air shower (80°). The neutrino-induced event candidates should exhibit the profile displayed in the top panel, but with a very inclined shower axis.

has conducted the searches for UHE neutrinos by looking for these deeply penetrating showers [13] or earth-skimming ν_τ-induced events [14].

Both the neutrino-induced deeply penetrating airshowers and the earth-skimming ν_τ events are identified by searching for very inclined (quasi-horizontal) showers in an early stage of cascade development. Filtering out non-horizontal events substantially reduces the background from UHECR-induced showers, the background events with large zenith angles remain to exist. These inclined showers induced by protons or nuclei in the upper atmosphere reach the ground as a thin and flat front of muons accompanied by an electromagnetic halo, which is produced by bremsstrahlung, pair production, and muon decays, and has a time structure very similar to that of the muons. On the other hand, if a shower is induced by a particle that interacts deep in the atmosphere (a deep neutrino interaction in air, or a tau decay), its electromagnetic component could hit the ground and give a distinct broad signal in time. The Auger surface detectors employ FADC electronics that allows one to trace the particles' hit-timing profile. Broad signals, which are characteristic as long as the electromagnetic component still develops, leave the larger ToT (Time Over Threshold) signature in the FADC traces. Fig. 5 displays examples of FADC traces. The ToT cut robustly gives the sample of the showers in an early stage of development ("young" showers). The inclination of events are estimated by the topology of the shower footprint that the triggered surface detector of the event leaves on the ground and the apparent speed with which the signal moves across the array. These variables are robust proxies of zenith angles, without relying on the high-level event reconstruction. The straight cuts on the ToT variables and the parameters associated with the footprint were used to search for earth-skimming events [28], while the Fisher discriminant methods on these multiple parameters was employed for searching for deeply penetrating downgoing young showers [13].

No events fulfilling the selection cuts are found in the dataset, leading to the upper limits of neutrino flux above 100 PeV. The limit from the ν_τ earth-skimming events is much more stringent than that by the deeply downgoing penetrating showers. The obtained bound is complementary to that obtained by the IceCube in the similar energy region. The limits from the various experiments are compiled and discussed in Section 5.

4. The UHE neutrino searches by measurements of impulsive radio emission

At PeV energies and above, UHE neutrinos can be detected in dense, radio-frequency (RF) transparent media via the Askaryan effect. Antarctic ice provides extremely low-loss transmission of RF signals. The charge asymmetry in the electromagnetic component of a high energy cascade induced by a UHE neutrino yields coherent, impulsive radio emissions. The amplitude of RF signals emitted by neutrino-generated electromagnetic showers in the MHz–GHz regime increases nearly linearly with energy, making radio detection cost-efficient and feasible at UHEs. The abundant cold ice covering Antarctica, with its exceptional RF clarity, has been host to the experiments designed to detect UHE neutrinos, including ANITA [15] and RICE [17].

ANITA searches for cascades initiated by a primary neutrino interacting in the Antarctic ice sheet within its field of view from the long-duration balloon altitude of 3537 km. Its target volume reaches $t \sim 10^6$ km^3. Although the low-duty cycle limits the resultant exposure to seek UHE neutrinos, ANITA has the greatest aperture for UHE neutrino detection in the

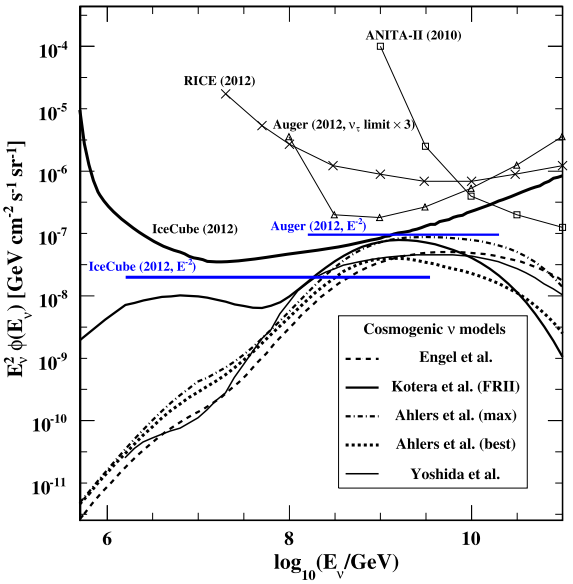

Fig. 6. (Color online.) All flavor neutrino flux differential 90% C.L. upper limit evaluated for each energy with a sliding window of one energy decade from the various experiments. Auger [14], RICE [17], ANITA [15,16], and IceCube [19], with appropriate normalization by taking into account the energy bin's width and the neutrino flavor. The upper limit for the ν_τ flux obtained by Auger is multiplied by 3 to convert it into an all-flavor neutrino flux limit (assuming an equal neutrino flavor ratio). Various model predictions (assuming primary protons) are shown for comparison; Yoshida et al. [5]. Engel et al. [11], Ahlers et al. [24], Kotera et al. [25].

10-EeV region. Its second Long Duration Balloon flight in January 2009 with 28.5 live days set the strongest limit of UHE neutrinos with energies greater than 10 EeV. RICE employs an array of radio sensors in the bulk of the polar ice. The radio receivers were deployed at a depth of 100–200 m from the ice surface. They seek the RF signals resulting from the collision of a neutrino with an ice molecule in the neighborhood of the deployed radio receiver array. Based on 12 years of data taken between 1999 and 2010, null observation of neutrino candidates resulted in the upper limit in the energy range from 0.1 to 100 EeV. The limits from ANITA and RICE are shown in Fig. 6.

The strategy of RICE is extendable: cost-effective growth of the radio receiver array will realize the Teraton scale of the target volume, large enough to bring excellent sensitivity in the heart of the GZK cosmogenic neutrino energy region (0.1–10 EeV). The Askaryan Radio Array (ARA) has been designed according to this principle [29]. The prototype detectors were deployed in 2011. More detector deployments are expected to follow for a next few years, yielding the sensitivity compatible with the present IceCube limit in year 2016 with $\sim 15\%$ of its full-scale array currently proposed. The full scale of ARA holds the promise for the most sensitive UHE neutrino detection.

5. The model-independent upper limits

Fig. 6 shows the quasi-differential, model-independent 90% C.L. upper limits on all flavor neutrino fluxes $\phi_{\nu_e+\nu_\mu+\nu_\tau}$. They were evaluated for each energy with a sliding window of one energy decade. An equal flavor ratio of $\nu_e : \nu_\mu : \nu_\tau = 1{:}1{:}1$ is assumed here. For the IceCube bound, the 90% event upper limit used in the calculation takes into account the energy PDFs of both observed PeV events. Any model predicting a neutrino flux above the bound curve is rejected at the 90% C.L. In the PeV region, the IceCube constraint is weaker, due to the detection of the two PeV events.

An IceCube upper limit for an E^{-2} spectrum that takes into account the two observed events was also derived and amounts to $E^2\phi_{\nu_e+\nu_\mu+\nu_\tau} = 2.5\times10^{-8}\ \mathrm{GeV\,cm^{-2}\,s^{-1}\,sr^{-1}}$ for an energy range of 1.6 PeV–3.5 EeV (90% event coverage) [19]. This is consistent with the estimated intensity by the follow-up analysis discussed in Section 2.3. The Auger limit for an E^{-2} spectrum is $E^2\phi_{\nu_e+\nu_\mu+\nu_\tau} \simeq 9.6\times10^{-8}\ \mathrm{GeV\,cm^{-2}\,s^{-1}\,sr^{-1}}$ in the energy range of 160 PeV–20 EeV (90% event coverage) [14].

6. Probing the UHECR origin with the cosmogenic neutrino models

The null observation of neutrinos with energies above 100 PeV by IceCube constrains the UHECR origin discussed in the literature. The intensity of the cosmogenic neutrinos in EeV is a good proxy to estimate the redshift distributions of the UHECR sources [9]. Bounding the intensity of neutrinos in EeV, thus, leads to constraints on the source evolution in the redshift space. It can then be compared with distributions of known classes of astronomical objects possibly responsible for UHECR emissions.

In order to set constraints on the redshift distributions of the UHECR sources, a parameterization often used in the literature [5] is employed, in which the spectral emission rate per co-moving volume scales as $(1+z)^m$ for $z \leqslant z_{\max}$. The

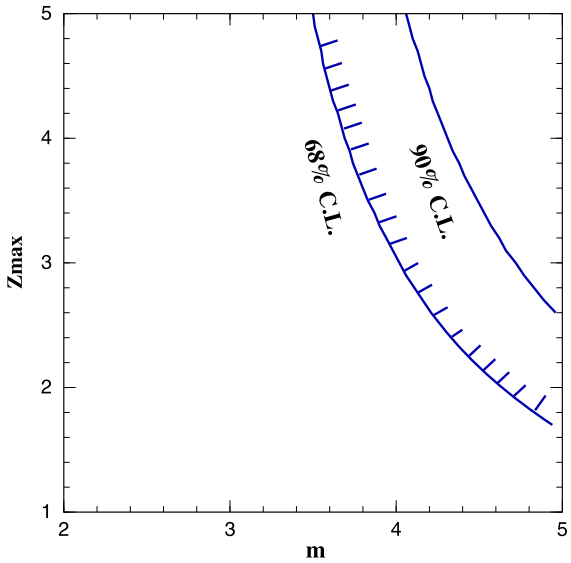

Fig. 7. (Color online.) Constraints on the UHECR source evolution parameters of m and $z_{\max}$ with the present analysis. The semi-analytic formulation [9] estimates the neutrino flux for calculating the limit shown here. The area above the solid lines is excluded at the quoted confidence level.

event rate at energies above 100 PeV is calculated for a given m, and $z_{\max}$ using the formula in Ref. [9]. The constraints on the parameter space of m and $z_{\max}$ are displayed in Fig. 7.

These studies indicates that strong source-evolution models ($m \gg 4$) are not responsible for the bulk of UHECRs. Among sources categorized in this class are the Fanaroff–Riley type-II (FR-II) radio galaxies, the long-standing favorite as a candidate of the UHECR emitters [30]. Similarly, a strong source evolution model for GRBs [31] is also rejected by our observation, since the model produces a higher neutrino flux than the FR-II model. This conclusion is universally valid because the cosmogenic neutrino intensity around 1 EeV, the central energy range of the presented search with IceCube, is stable against uncertainties in the IR/UV backgrounds and the transition model between the galactic and extragalactic component of the UHECRs [9,25,26,32,33].

The present constraint also excludes the flux level maximally allowed by the diffuse photon flux. It demonstrates that the present constraints from the limit on the ultra-high-energy neutrino flux are compatible with those from photon flux measurements by Fermi in the 10 GeV region [34]. These constraints are highly complimentary to the constraints from the diffuse photon flux [24,34], because the former does not rely on uncertain estimation of magnetic fields and extra-galactic background light (EBL).

We should note, however, that the obtained bound is not valid if the mass composition of UHECRs is not dominated by proton primaries. The dominance of proton primaries is widely assumed in the models mentioned here, while a dominance of heavier nuclei such as iron provides at least 2–3 times lower neutrino fluxes. The neutrino analysis with the present detectors is not sensitive enough to reach these fluxes yet.

7. Summary

The detection of PeV neutrinos demonstrated that the neutrino channel may open a path to identify the sources of cosmic rays. The detection sensitivity of UHE neutrinos has been rapidly improved over the last decade and now reached $O(10^{-8})$ GeV cm^{-2} s^{-1} sr^{-1} from PeV to 100 EeV by the IceCube, Auger, and ANITA experiments. Because this level of flux has been naturally expected from the arguments of the energetics and/or intensity of the observed UHECRs, the on-going neutrino observations provide the characteristics of UHECRs without relying on uncertain factors such as the (inter-)galactic magnetic field or the EBL spectrum, as discussed above. The future projects such as ARA whose sensitivity enters the domain of $O(10^{-9})$ GeV cm^{-2} s^{-1} sr^{-1} will scan most of the parameter space regarding the UHECR emitters even if they are dominated by heave nuclei.

Another possible way to probe the UHECR origin with neutrinos is the multi-messenger approach, the simultaneous observations with the photon channels such as the GeV–TeV gamma-rays. The neutrino channel enables us to identify a domain of the sky emitting UHECRs in realtime manner. One or more follow-up observation(s) with gamma-ray and optical telescopes is capable of pinning down the source object with their excellent pointing accuracy. The multi-messenger campaign has been initiated among the neutrino telescopes and the gamma-ray/optical observatories. The next decade will be an interesting time window to see any outputs from this strategy.

Acknowledgements

We wish to acknowledge Antoine Letessier-Selvon for his kind invitation to contribute to this dossier of the Comptes rendus Physique. This work was supported in part by the Grants-in-Aid in Scientific Research from the JSPS in Japan (grant number 25220706).

References

[1] J.N. Bahcall, et al., Astrophys. J. 626 (2005) 530.
[2] S. Ando, Astrophys. J. 607 (20) (2004).
[3] R. Abbasi, et al., IceCube Collaboration, Phys. Rev. D 84 (2011) 082001.
[4] E. Waxman, J. Bahcall, Phys. Rev. D 59 (1998) 023002.
[5] S. Yoshida, M. Teshima, Prog. Theor. Phys. 89 (1993) 833.
[6] K. Greisen, Phys. Rev. Lett. 16 (1966) 748.
[7] G. Zatsepin, V. Kuzmin, JETP Lett. 4 (1966) 78.
[8] V. Berezinsky, G. Zatsepin, Phys. Lett. B 28 (1969) 423.
[9] S. Yoshida, A. Ishihara, Phys. Rev. D 85 (2012) 063002.
[10] M. Ahlers, L.A. Anchordoqui, S. Sarkar, Phys. Rev. D 79 (2009) 083009.
[11] R. Engel, D. Seckel, T. Stanev, Phys. Rev. D 64 (2001) 093010.
[12] X. Bertou, et al., Astropart. Phys. 17 (2002) 183.
[13] P. Abreu, et al., Pierre Auger Collaboration, Phys. Rev. D 84 (2011) 122005.
[14] P. Abreu, et al., Pierre Auger Collaboration, Astrophys. J. 755 (2012) L4.
[15] P.W. Gorham, et al., ANITA Collaboration, Phys. Rev. D 82 (2010) 022004.
[16] P.W. Gorham, et al., ANITA Collaboration, Phys. Rev. D 85 (2012) 049901.
[17] I. Kravchenko, et al., Phys. Rev. D 85 (2012) 062004.
[18] A. Achterberg, et al., IceCube Collaboration, Astropart. Phys. 26 (2006) 155.
[19] M.G. Aartsen, et al., IceCube Collaboration, Phys. Rev. D 88 (2013) 112008.
[20] G.C. Hill, et al., in: Proceedings of PHYSTAT2005, Oxford, 2006, p. 108.
[21] R. Abbasi, et al., IceCube Collaboration, Phys. Rev. D 83 (2011) 092003.
[22] M. Aartsen, et al., IceCube Collaboration, Phys. Rev. Lett. 111 (2013) 021103.
[23] R. Enberg, M.H. Reno, I. Sarcevic, Phys. Rev. D 78 (2008) 043005.
[24] M. Ahlers, et al., Astropart. Phys. 34 (2010) 106.
[25] K. Kotera, D. Allard, A. Olinto, J. Cosmol. Astropart. Phys. 1010 (2010) 013.
[26] V.S. Berezinsky, A. Gazizov, S. Grigorieva, Phys. Rev. D 74 (2006) 043005.
[27] M. Aartsen, et al., IceCube Collaboration, Science 342 (2013) 1242856.
[28] J. Abraham, et al., Pierre Auger Collaboration, Phys. Rev. D 79 (2009) 102001.
[29] P. Allison, et al., ARA Collaboration, Astropart. Phys. 35 (2012) 457.
[30] P. Biermann, P. Strittmatter, Astrophys. J. 322 (1987) 643.
[31] H. Yuksel, M.D. Kistler, Phys. Rev. D 75 (2007) 083004.
[32] H. Takami, K. Murase, S. Nagataki, K. Sato, Astropart. Phys. 31 (2009) 201.
[33] G. Decerprit, D. Allard, Astron. Astrophys. 535 (2011) A66.
[34] V. Berezinsky, A. Gazizov, M. Kachelriess, S. Ostapchenko, Phys. Lett. B 695 (2011) 13.